Received: 21 March 2017 | Accepted: 18 January 2018 | Published on: 25 March 2018

DOI: 10.1002/asna.201813369

ORIGINAL ARTICLE

Astronomische Nachrichten

Spectral evolution of the two classical novae PW Vul and V1668 Cyg using International Ultraviolet Explorer low-resolution spectra

G. M. Hamed[1,*] | M. R. Sanad[1] | S. Yousef[2] | A. Essam[1] | M. El Rafy[2]

[1]Stellar Astronomy Lab, Astronomy Department, National Research Institute of Astronomy and Geophysics, Helwan, Egypt

[2]Department of Astronomy, Space Science and Meteorology, Cairo University, Giza, Egypt

***Correspondence**

G. M. Hamed, Stellar Astronomy Lab, Astronomy Department, National Research Institute of Astronomy and Geophysics, 11421 Helwan, Cairo, Egypt.

Email: gamal.hamed@nriag.sci.eg

We studied the evolution of the normalized flux of selected ultraviolet (UV) emission lines of two classical novae (PW Vul and V1668 Cyg) using International Ultraviolet Explorer (IUE) short wavelength observations. Different phases of the outburst are studied. Emission lines covering a wide range of ionization states are investigated. We use the calculated fluxes to estimate the mass accretion rates during quiescence of both novae. We found average values of the UV luminosity for PW Vul to be of $1.0 \pm 0.1 \times 10^{35}$ erg s^{-1}, and the corresponding value for V1668 Cyg is $4.0 \pm 0.2 \times 10^{35}$ erg s^{-1}. In quiescence, we obtained average values for the mass accretion rates $\dot{M}_{\rm acc}$ of $8.7 \pm 0.4 \times 10^{-10}\ M_{\odot}$ year^{-1} and $1.8 \pm 0.1 \times 10^{-10}\ M_{\odot}$ year^{-1}, respectively. We attribute the spectral behavior of the two systems to the variation of the optical thickness and temperature of the envelope during the different phases of the outburst. Our results demonstrate the effect of the white dwarf mass on the evolution of the nova. The results of IUE observations are consistent with the theoretical CO models of classical nova of.

KEYWORDS

novae, cataclysmic variables – stars: Individual (V1668 Cyg, PW Vul) – ultraviolet: stars – white dwarfs

1 | INTRODUCTION

Cataclysmic variables (CVs) are semidetached binary stars consisting of a white dwarf (WD) accreting matter from a late-type main sequence star via Roche lobe overflow.

CVs are characterized by sudden eruptions, called classical nova outbursts, during which the system brightness increases by 6 mag, up to 19 mag, from the prenova state. It is widely accepted that this outburst is due to a thermonuclear runaway of the matter accreted onto the surface of the WD (Warner 2003). It has been proposed that, after the explosion, part of the mass accreted on the surface of the WD is then ejected in the form of an optically thick wind (e.g., Bath 1978; Kato & Hachisu 1994), where most of the mass of the envelope is lost during this phase. Novae are usually classified according to their fading rate in various speed classes depending on the time required for a nova to decline 3 mags below its visual maximum (t_3). Very fast novae have t_3 shorter than 15 days, fast novae have $t_3 \simeq 15$–45 days, average novae have $t_3 \simeq 50$–85 days, and slow novae have t_3 longer than 85 days (Duerbeck 2008; Mclaughlin 1945).

The study of classical novae in outburst has great importance in astrophysics as it helps in understanding the nature of WDs, the evolution of binary systems, thermonuclear runaway processes, and the hydrodynamics of the explosion. This is because it is possible to determine the mass, surface temperature, and core composition of the WD, as well as the dynamics and the chemical abundances of the ejecta, by studying the nova outburst during different phases.

The evolution of the spectrum of a classical nova during the outburst passes through different stages (Cassatella et al. 2005; Schwarz et al. 2001; Shore 2008, 2012; Shore et al. 1994). The first one is the "fireball" phase, which appears with an explosion as the ejecta are heated by the resulting shock. This phase, characterized by the high optical thickness of the ejecta in both the continuum and the lines, is

TABLE 1 Journal of IUE observations for PW Vul

Spectrum ID	JD −2440000	Days after explosion	Exposure time (s)	Spectrum ID	JD −2440000	Days after explosion	Exposure time (s)
SWP23577LL	5915.0	7	1500	SWP24473LL	6018.2	110	600
SWP23580LL	5915.3	7	1200	SWP25622LL	6163.2	255	1200
SWP23603LL	5917.9	10	900	SWP25623LL	6163.3	255	300
SWP23604LL	5917.9	10	720	SWP26243LL	6241.1	333	360
SWP23605LL	5918.0	10	810	SWP26244LL	6241.1	333	1200
SWP23638LL	5920.3	12	2100	SWP26342LL	6249.6	342	2219
SWP23675LL	5924.9	17	2519	SWP26427LL	6263.2	355	600
SWP23717LL	5930.8	23	99	SWP26470LL	6271.6	364	1080
SWP23825LL	5943.3	35	1800	SWP26997LL	6367.8	460	900
SWP23837LL	5944.9	37	300	SWP28068LL	6521.0	613	4199
SWP23860LL	5947.0	39	300	SWP28461LL	6591.0	683	4199
SWP24072LL	5972.6	65	600				

TABLE 2 Journal of IUE observations for V1668 Cyg

Spectrum ID	JD −2440000	Days after explosion	Exposure time (s)	Spectrum ID	JD −2440000	Days after explosion	Exposure time (s)
SWP02636LL	3764.2	5.0	1500	SWP03136LL	3806.9	48	150
SWP02641LL	3765.0	6.0	1200	SWP03169LL	3808.9	50	180
SWP02653LL	3767.0	8.0	1200	SWP03182LL	3810.8	52	180
SWP02655LL	3767.2	8.0	2099	SWP03190LL	3811.4	52	360
SWP02666LL	3768.6	10.0	900	SWP03203LL	3813.8	55	180
SWP02679LL	3769.9	11.0	1200	SWP03238LL	3819.3	60	540
SWP02680LL	3767.0	11.0	600	SWP03274LL	3821.6	63	150
SWP02697LL	3771.3	12.0	119	SWP03362LL	3829.1	70	540
SWP02702LL	3771.7	13.0	1800	SWP03375LL	3830.8	72	292
SWP02703LL	3771.8	13.0	300	SWP03526LL	3847.2	88	540
SWP02727LL	3773.8	15.0	1800	SWP03532LL	3847.8	89	720
SWP02734LL	3774.6	16.0	1380	SWP03714LL	3869.2	110	720
SWP02742LL	3775.5	16.0	180	SWP03886LL	3885.2	126	180
SWP02752LL	3776.6	18.0	1200	SWP03908LL	3887.0	128	2400
SWP02795LL	3779.9	21.0	900	SWP04505LL	3938.7	180	600
SWP02820LL	3782.9	24.0	480	SWP04637LL	3947.7	189	180
SWP02883LL	3789.8	31.0	119	SWP04720LL	3954.4	195	1620
SWP02884LL	3789.9	31.0	480	SWP04737LL	3956.8	198	1500
SWP02902LL	3792.4	33.0	540	SWP05755LL	4063.5	305	18,000
SWP02966LL	3795.6	37.0	96	SWP06077LL	4090.7	332	14,400
SWP02990LL	3797.4	38.0	60	SWP07621LL	4248.3	489	14,400
SWP03011LL	3799.3	40.0	300	SWP09065LL	4380.7	622	23,700
SWP03089LL	3803.4	44.0	96	SWP09079LL	4382.7	624	24,780
SWP03134LL	3806.8	48.0	150	SWP10886LL	4598.6	840	21,600

rarely observed as it lasts for a very short time, typically a few days. Then, the "iron curtain" phase follows, during which the ejecta cool down, and iron peak elements start to recombine and blanket the spectrum. The third phase, known as "lifting the iron curtain," is characterized by the decrease in the opacity of the ultraviolet (UV) lines in the envelope. In this phase, the pseudophotosphere pulls back toward hotter regions, enhancing the ionization, and the absorption lines in the UV disappear. Cassatella et al. (2005) found that this phase ends $\simeq 1.1t_3$ after the visual maximum in novae, occurring in WDs with carbon–oxygen cores. Then, the nova spectrum evolves into the "pre-nebular" or "transition" phase, which is characterized by the appearance of semiforbidden lines and the decrease of the opacity of the ejecta. The emission arises now from low-density regions as can be seen in the increasing strength of the C III] line. The maximum flux of the C III] line marks the end of this phase, usually about $2.45t_3$ days after the visual maximum. The final phase is the "nebular" phase, during which the spectrum shows strong forbidden emission lines (such as [O I], [N II], and [O III]), and

the emission lines of high ionization states (e.g., C IV and N V) reach their maximum flux. Then, the spectrum returns to its prenova appearance.

The UV spectra of novae contain a wide range of intercombination, resonance, and forbidden lines of many elements. As different emission lines are characteristic of different phases of the outburst, their study allows us to accurately determine the physical conditions and chemical abundances of the ejecta (González-Riestra & Krautter 1998). The evolutionary curves of different UV emission lines determine the times when the nova enters different phases of the outburst. Mass accretion rate can be determined from the study of the accretion luminosity determined from the UV line fluxes in the quiescent phase.

José & Hernanz (1998) developed a hydrodynamical model to follow the progress of a nova outburst from the accretion stage up to the explosion. The input parameters of the model are the WD mass (ranging from 0.8 to 1.15 $M_{\odot}$ for carbon–oxygen core (CO) models and from 1.0 to 1.35 $M_{\odot}$ for oxygen–neon core (ONe) models) and the mixing ratio of the elements between the core and the envelope (ranging from 25 to 75%). The mass of the accreted envelope, the mass of the ejected envelope, the ejection speed, and the duration of the accretion process are among the main outputs of the model. Each model also determines the chemical composition of the ejecta (José & Hernanz 1998, see their tables 2 and 4).

In this paper, we present UV observations of two classical novae (PW Vul & V1668 Cyg) obtained with the International Ultraviolet Explorer (IUE) satellite following their spectral evolution after the nova events. The spectra and data reduction are presented in Section 2. Section 3 summarizes our main results: from the analysis of the evolution of the normalized fluxes of selected emission lines, we calculate the UV luminosities, which, in turn, provide the mass accretion rates of the two novae in quiescence. A discussion of the results is presented in Section 4, while the main conclusions are listed in Section 5.

2 | OBSERVATIONS AND DATA REDUCTION

IUE low-resolution short wavelength (1150–2000 $\AA$) spectra are used in this paper. All the spectra were acquired with the short wavelength prime camera with low dispersion (this mode uses a cross-disperser grating yielding a ∼6 $\AA$ resolution) and large aperture (a 10×20 arcsecond slit). The files were retrieved through the INES (IUE newly extracted spectra) server at http://sdc.cab.inta-csic.es/ines/.

IUE observations of PW Vul are listed in Table 1. These observations were obtained in the period between 12/08/84 and 09/06/86. V1668 Cyg observations cover the period between 11/09/78 and 24/12/80. The log of the observations is reported in Table 2. Sample spectra for both systems are presented in Figures 1–4. Making use of the quality

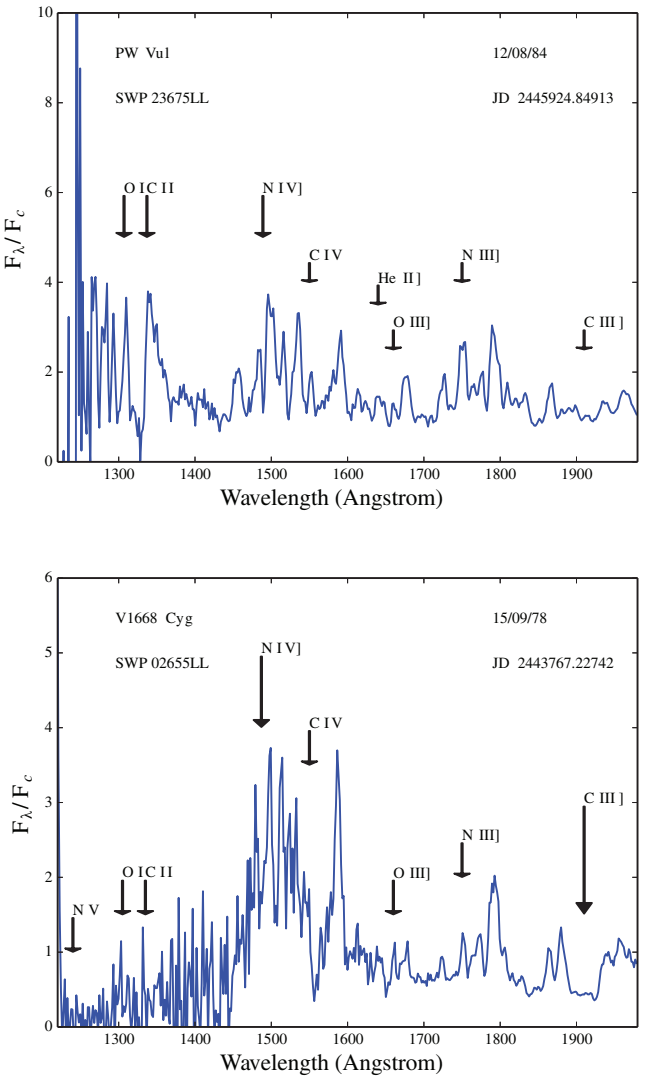

FIGURE 1 PW Vul lifting the iron curtain phase (top); V1668 Cyg lifting the iron curtain phase (bottom). Note the presence of emission lines while the continuum is strong and the semiforbidden and forbidden lines are weak

column in the FITS files of the spectra and following the guidance of Loiseau & Solano (1998, see their table 1), we inspected each spectrum by eye and discarded those with high noise.

Image Reduction and Analysis Facility (IRAF) version 2.16 was used to normalize the spectra and measure the line fluxes. The continuum level was best fitted using a fifth-order Chebyshev function, which was then used to normalize the spectrum. The properties of the emission lines were then measured interactively using the splot task of the onedspec package; by performing a Gaussian fit to each of the selected lines, we determined their maximum flux and width.

3 | RESULTS

3.1 | PW Vul

PW Vul (Nova Vul 1984a) was discovered in outburst on July 28, 1984 (JD 2445910), and it reached its visual maximum

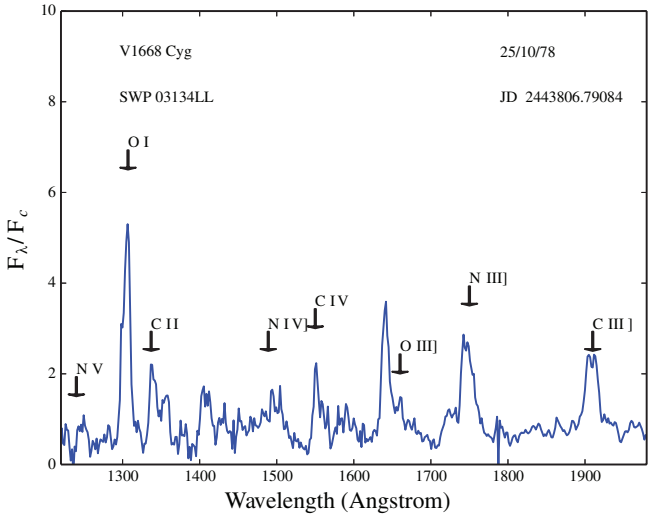

FIGURE 2 V1668 Cyg prenebular phase. Semiforbidden lines start to appear. The prenebular phase of PW Vul was not observed

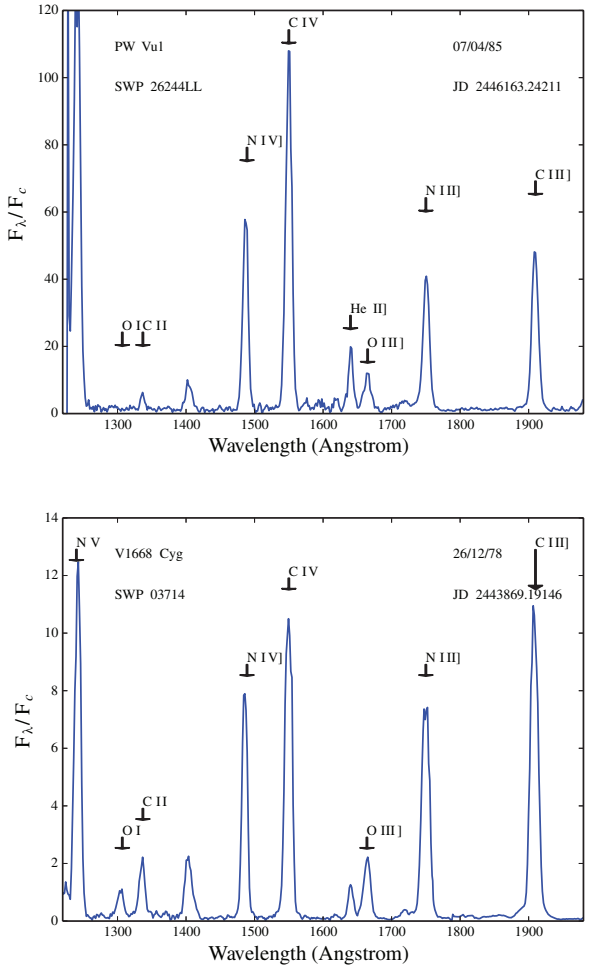

FIGURE 3 PW Vul nebular phase (top) and V1668 Cyg nebular phase (bottom). Semiforbidden lines and lines from high ionization species are strong

7 days later (Cassatella et al. 2005; Gehrz et al. 1988; Kosai et al. 1984). Its V-band magnitude at discovery was 9.2 mag, and it reached 6.3 mag at maximum (Andreae et al. 1991). Hachisu & Kato (2014) assumed that the outburst occurred on JD 2445908.0 (UT July 26, 1984.5). Gehrz et al. (1988) report a t_3 time of 100 days, making PW Vul a slow nova. Downes & Duerbeck (2000) used the expansion parallax method to obtain a distance of 1.8 ± 0.05 kpc. We adopted this value, with $E(B-V) = 0.55$ mag (Downes & Duerbeck 2000; Hachisu & Kato 2015).

The emission lines seen in the UV spectra of PW Vul cover a wide range of ionization states and ionization potentials from 13.60 eV for O I to 47.98 eV for C IV. In this paper, we studied the C IV 1550 $\AA$ resonance emission doublet, the O I 1306 $\AA$ collisionally excited resonance triplet pumped by Hydrogen Lyman β, and the N IV] 1487 and C III] 1909 $\AA$ intercombination lines.

The normalized line fluxes (F_λ/F_c) are plotted as a function of Julian date in Figure 5a–d. We used these fluxes to calculate the luminosities of the spectral lines using the equation

$$L_\lambda = 4\pi F_\lambda d^2. \tag{1}$$

We corrected F_λ for interstellar extinction using the relationship:

$$F = F_o 10^{0.4X(\lambda)E(B-V)} \tag{2}$$

from Stickland et al. (1981), where F_o is the observed unnormalized flux, and $X(\lambda)$ is the analytic function fitted by Seaton (1979) for the interstellar extinction in the UV. Maximum, intermediate, and minimum luminosity values are listed in Table 3. We consider that the system has entered the quiescent stage for the last two spectra (SWP28068LL ans SWP28461), when the flux of the continuum and emission lines have decreased to 0.2% and less than 3% of the maximum values, respectively.

Our assumption is consistent with the model of Hachisu & Kato (2015) where they assumed that the wind stopped about 620 days after the outburst (marked by the dotted line in Figure 5a–d, which lies between the last two spectra). We then used the quiescent luminosity to calculate the mass accretion rate onto the WD $\dot{M}_{\rm acc}$ using the equation

$$\dot{M}_{\rm acc} = \frac{L_{\rm acc} R_{\rm WD}}{G M_{\rm WD}}, \tag{3}$$

where G is the universal gravitational constant, and $M_{\rm WD}$ is the mass of the WD ($= 0.83\,M_\odot$ as derived by Hachisu & Kato 2015). $R_{\rm WD}$ is the radius of the WD calculated using the mass–radius relationship from Nauenberg (1972):

$$R_{\rm WD} = 0.78 \times 10^9 \left[\left(\frac{1.44 M_\odot}{M_{\rm WD}} \right)^{2/3} - \left(\frac{M_{\rm WD}}{1.44 M_\odot} \right)^{2/3} \right]^{1/2}. \tag{4}$$

The radius of the WD was found to be $0.0097\,R_\odot$.

The normalized flux of all emission lines generally start at relatively low values and increases gradually to reach maxima on JD 2446018, 101 days after the visual maximum for O I line. The C III], C IV, and N IV] lines reach maxima on JD

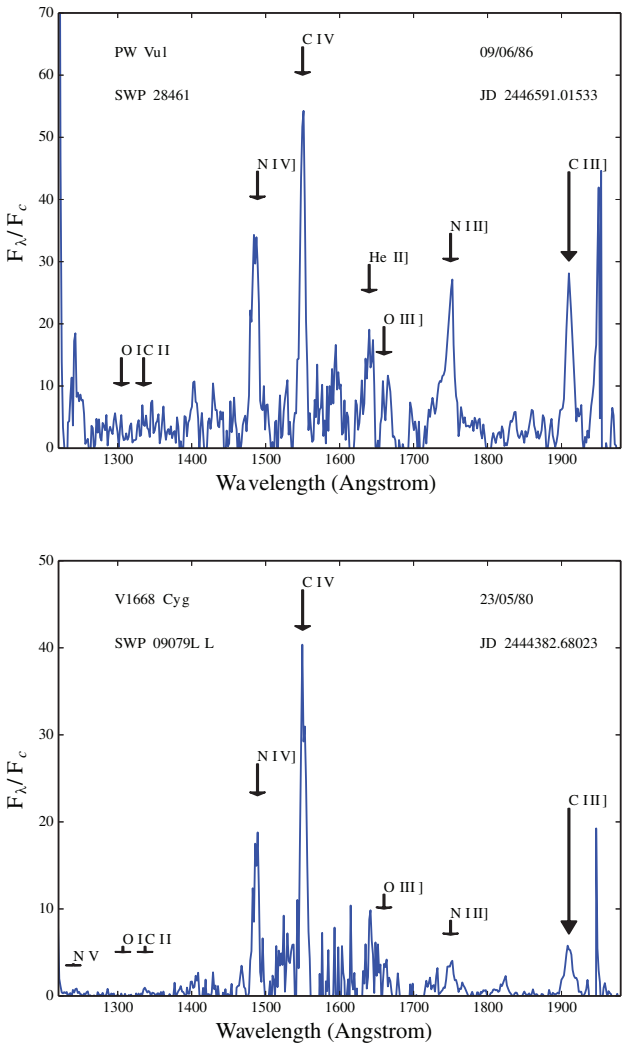

FIGURE 4 PW Vul quiescent phase (top) and V1668 Cyg quiescent phase (bottom)

2446163, 246 days after the visual maximum. This behavior can be seen in Figure 5a–d.

3.2 | V1668 Cyg

V1668 Cyg (Nova Cygni 1978) was discovered in outburst on JD 2443762 with a visual magnitude of 6.2 (Morrison et al. 1978). At maximum, it reached a visual magnitude of 6.0 mag on JD 2443764 (Andrews et al. 1978). Gehrz et al. (1980) estimated the outburst day to be JD 2443759.0. Duerbeck et al. (1980) report a t_3 time of 23 days, making V1668 Cyg a fast nova.

For V1668 Cyg, we studied the C IV 1550 Å, O I 1306 Å, N III] 1750 Å, and the N V 1240 Å resonance line. The emission line with the highest ionization potential was the N V resonance line at 1240 Å with 77.47 eV. The normalized line fluxes for all the studied emission lines are plotted as a function of Julian date in Figure 7a–d.

We calculated the line luminosities for V1668 Cyg using Equation 1 assuming a distance of 3.3 ± 0.6 kpc and $E(B-V) = 0.38$ mag, as derived by Slovak & Vogt (1979). Maximum, intermediate, and minimum luminosity values are listed in Table 4.

The normalized fluxes of different emission lines show similar behaviors, generally starting at relatively low values and then increasing gradually toward the maximum, as can be seen in Figure 7a–d. The maximum value is reached at different days after the visual maximum for different ionized species: 59 days (JD 2443821) for O I, 85 days (JD 2443847) for N III], 123 days (JD 2443885) for N V, and 176 days (JD 2443938) for C IV. However, in the quiescent phase (on JD 2444382), we measured a value for the C IV normalized flux that was higher than the value we measured on JD 2443938. This behavior can be seen in Figure 7a–d.

4 | DISCUSSION

4.1 | PW Vul

In a previous study of the same IUE data, Cassatella et al. (2005) obtained a similar trend for the evolution of the line fluxes of the O I and C III] lines (see Figure 5a and b from this work and fig. 2 from Cassatella et al. 2005). Moreover, most of the measured line fluxes determined here are consistent with the fluxes measured by Andreae et al. (1991) for the nebular phase spectra.

Studying the evolution of the UV spectrum of PW Vul, Cassatella et al. (2005) found that the "lifting the iron curtain" phase (which they called "initial phase") ended about 100 days after the visual maximum, when the O I line reaches its maximum flux, while the prenebular phase ended about 250 days after the visual maximum with the maximum flux of the C III] line. Our results are consistent with these two findings. The third and final phase they studied was the nebular phase.

During the initial phase, the decrease in the opacity and the increase in the temperature lead to the gradual increase of the flux of the O I line until it reaches its maximum by the end of this phase. The decrease in the density and the opacity of the ejecta in the prenebular phase enhances the emission of the C III] line. The maximum of the lines of high ionization states (N IV and C IV), in the nebular phase, demonstrates that the density and the opacity are now low enough for these species to reach their maximum fluxes.

We present the evolution of the fitted continuum flux in the whole wavelength range in Figure 6, where it can be seen that the evolution curve reached the maximum at JD 2445987 ± 23, which is consistent with the evolution curve of the continuum at 1455 Å from Cassatella et al. (2002). This lags $\simeq$ 70 days after the visual maximum, which means that the maximum light is shifting toward higher energies.

We also calculate the expansion velocity of the nova by measuring the widths of the spectral lines. We find an average value of $\sim$1300 km s^{-1}, which is slightly higher than the average ejection speed of the CO2 model (1200 km s^{-1})

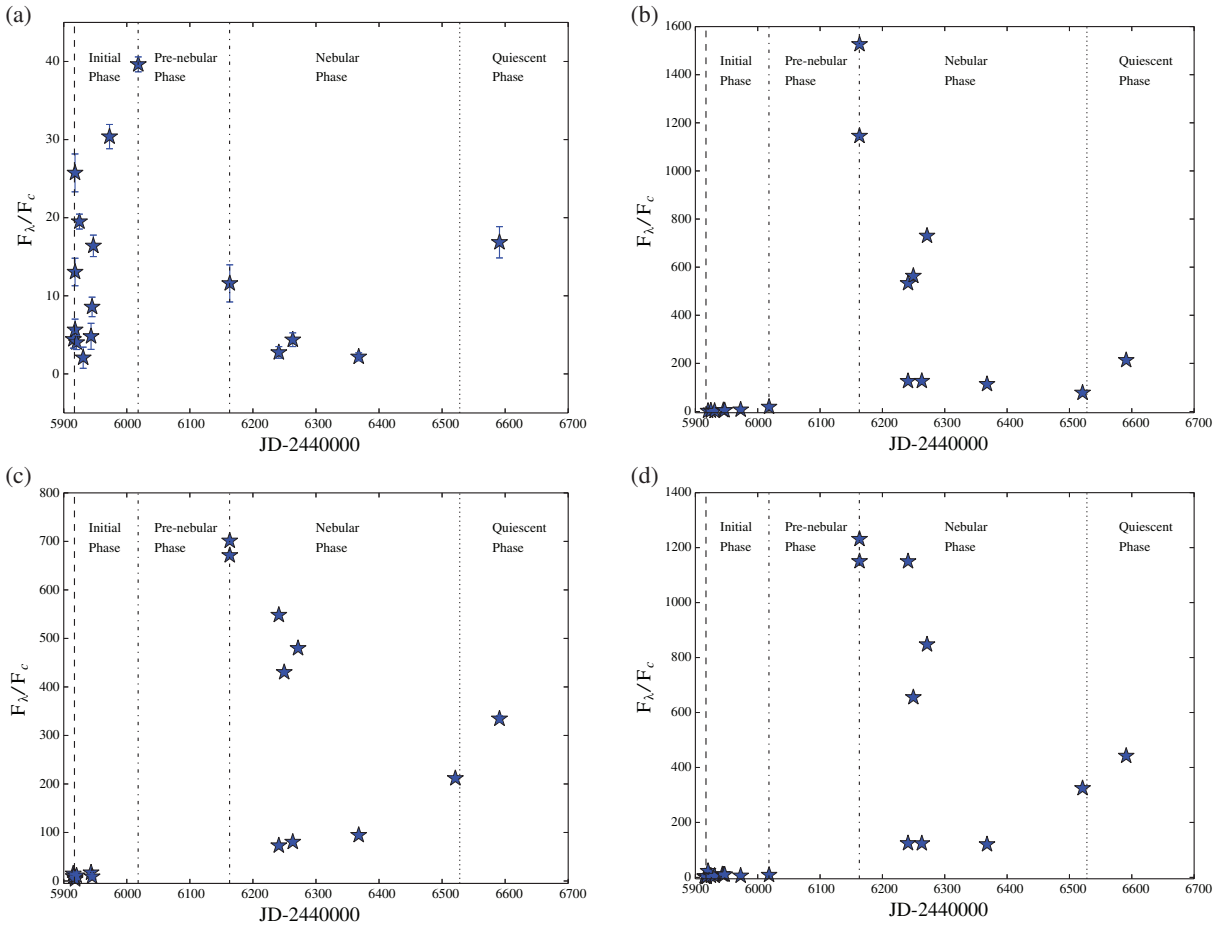

FIGURE 5 PW Vul line spectral evolution. The dashed line represents the time of visual maximum and the dash–dotted lines represent the end of the different phases of evolution. (a) O I; (b) C III; (c) N IV; and (d) C IV

of José & Hernanz (1998). This value is different from the value of 750 km s^{-1} reported by Cassatella et al. (2005), while it is in agreement with the expansion velocities reported by Cassatella & Gonzalez Riestra (1988), 0, 750, and 1550 km s^{-1}).

During the early phases of the outburst, the mass accretion process of the WD is greatly reduced and only starts to become significant in the quiescent stage (Hachisu & Kato 2006). We therefore measured the mass accretion rate ($\dot{M}_{\rm acc}$) from the last two spectra corresponding to the quiescent phase. The mass accretion rate determined from the C IV line on JD 2446367 about 611 days after the outburst results in $\dot{M}_{\rm acc} = 1.7 \pm 0.1 \times 10^{-9} M_\odot$ year^{-1}, while the average value obtained using all the studied emission lines is $\dot{M}_{\rm acc} = 8.7 \pm 0.4 \times 10^{-10} M_\odot$ year^{-1}. This latter value suggests a recurrence time of $\simeq 1 \times 10^5$ years, which is slightly smaller than the accretion time for the CO2 model calculated by José & Hernanz (1998) for novae of similar WD mass and expansion speed. The expansion velocity, the accretion rate, and the recurrence time we determined for PW Vul are consistent with the CO2 model by José & Hernanz (1998).

TABLE 3 PW Vul emission line parameters. (F_λ/F_c) is the normalized flux, F_λ is the absolute flux, and L is the luminosity. Intermediate values are the mean of all the values calculated for a specific parameter

Value	O I	C III]	N IV	C IV
$(F_\lambda/F_c)_{\rm max}$	40 ± 1	1527 ± 5	701 ± 2	1231 ± 4
$F_{\lambda({\rm max})}$ (10^{-09} erg cm^{-2} s^{-1} Å^{-1})	1.92 ± 0.05	1.265 ± 0.002	1.39 ± 0.01	2.099 ± 0.006
$L_{\rm max}$ (10^{35} erg s^{-1})	7.4 ± 0.3	4.9 ± 0.2	5.4 ± 0.2	8.1 ± 0.3
$(F_\lambda/F_c)_{\rm mid}$	9 ± 1	113.7 ± 0.8	80 ± 1	11 ± 1
$F_{\lambda({\rm mid})}$ (10^{-11} erg cm^{-2} s^{-1} Å^{-1})	2.0 ± 0.1	22 ± 3	15 ± 2	15 ± 1
$L_{\rm mid}$ (10^{34} erg s^{-1})	0.078 ± 0.005	9 ± 1	5.8 ± 0.7	5.7 ± 0.6
$(F_\lambda/F_c)_{\rm min}$	2 ± 1	2.3 ± 0.9	3 ± 1	2 ± 1
$F_{\lambda({\rm min})}$ (10^{-12} erg cm^{-2} s^{-1} Å^{-1})	2.9 ± 0.4	8 ± 4	0.8 ± 0.5	7 ± 3
$L_{\rm min}$ (10^{33} erg s^{-1})	1.1 ± 0.2	3 ± 1	0.3 ± 0.2	3 ± 1

TABLE 4 V1668 Cyg emission line parameters. See Table 3 caption

Value	O I	N III]	C IV	N V
$(F_\lambda/F_c)_{max}$	55.5 ± 0.3	107.5 ± 0.2	294 ± 6	142 ± 1
$F_{\lambda(max)}$ (10^{-09} erg cm^{-2} s^{-1} Å^{-1})	1.70 ± 0.04	1.78 ± 0.02	1.68 ± 0.01	0.896 ± 0.007
L_{max} (10^{36} erg s^{-1})	2.21 ± 0.05	2.32 ± 0.03	2.19 ± 0.02	1.17 ± 0.01
$(F_\lambda/F_c)_{mid}$	32.4 ± 0.6	43.6 ± 0.6	8.7 ± 0.8	20.5 ± 0.2
$F_{\lambda(mid)}$ (10^{-10} erg cm^{-2} s^{-1} Å^{-1})	7.9 ± 0.3	1.4 ± 0.2	1.4 ± 0.2	2.9 ± 0.2
L_{mid} (10^{35} erg s^{-1})	10.3 ± 0.4	1.8 ± 0.3	1.9 ± 0.2	3.7 ± 0.2
$(F_\lambda/F_c)_{min}$	1.2 ± 0.2	2 ± 1	4.7 ± 0.8	2.4 ± 0.1
$F_{\lambda(min)}$ (10^{-13} erg cm^{-2} s^{-1} Å^{-1})	2 ± 1	3.4 ± 0.3	17.8 ± 0.3	17 ± 2
L_{min} (10^{32} erg s^{-1})	2 ± 1	4.5 ± 0.4	23.1 ± 0.4	22 ± 3

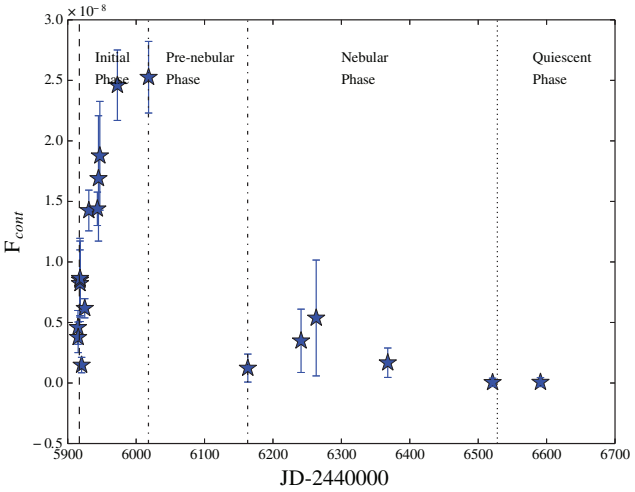

FIGURE 6 PW Vul continuum evolution. See Figure 5a caption

José & Hernanz's (1998) model calculated the abundances of different elements in the ejecta a few days after the nova outburst. They identify PW Vul as a CO4 nova based on the agreement between the results of the model and the abundances calculated by Andreae et al. (1991) using the nebular phase spectra and those calculated by Andrea et al. (1994) using observations taken about 180 days after the outburst. There is a difference between the model we identify for PW Vul and the model identified by José & Hernanz (1998). This difference probably arises from the fact that the model predicts the chemical composition few days after the outburst, while the abundances calculated in the previously mentioned papers were based on observations taken in later stages of the outburst. This difference may be resolved if the model can predict the abundances in the ejecta in the nebular phase, when the abundances can be determined from nebular line analysis.

4.2 | V1668 Cyg

The evolution curve of the normalized fluxes for the O I, N III], and N V lines (Figure 7a–d) demonstrated the same trend reported by Cassatella et al. (2005, their fig. 1). Moreover, our results are in good agreement with the values determined by Stickland et al. (1981) during the nebular phase.

During the initial phase, the decrease in the opacity and the increase in the temperature lead to the gradual increase of the flux of the O I line until it reaches its maximum by the end of this phase. The emission of the N III] semiforbidden line is enhanced by the decrease of both the density and the opacity in the ejecta in the prenebular phase until the flux reaches its maximum in the beginning of the nebular phase. During the nebular phase, the density and opacity are low enough for the fluxes of emission lines with high ionization states to reach their maxima. This can be seen in the evolutionary curves of C IV and N V lines.

The evolutionary curve of the fitted continuum is presented in Figure 8, and it can be seen that it reaches the maximum on JD 2443790 ± 9, which is consistent with evolution of the continuum at 1455 Å presented by Cassatella et al. (2002). This occurs ≃26 days after the visual maximum, which means that the maximum light has shifted from the optical toward the UV.

By measuring the widths of the spectral lines, we calculated the expansion velocities of the nova, finding an average value of ∼1800 km s^{-1}, which is close to the average ejection velocity of the CO3 model of José & Hernanz (1998). Cassatella et al. (1979) reported a value of 1160 km s^{-1} for the expansion velocity. This difference is due to the different method they used, where they calculated this value from the blue shift of the absorption component of the P Cygni profile of Mg II line. Although using the P Cygni profile can be a more reliable method to measure the expansion velocity, we favor our results as the 1160 km s^{-1} value was measured on only 1 day of the observations, while our value was calculated based on averaged values through all the stages of the outburst.

Cassatella et al. (2005) found that the initial phase ended on JD 2443799 and that the prenebular phase ended at JD 2443830. The system then entered the quiescent (postnova) phase on JD 2444090, as can be seen from the drop in the continuum and emission line flux in the IUE observations.

Hachisu & Kato (2006) assumed that the wind stops ∼ 280 days after the outburst (marked by the dotted line in Figure 7a–d), that is, about 50 days before the last observation available in the nebular phase. We considered that the system has entered the quiescent (post-nova) phase for the final four

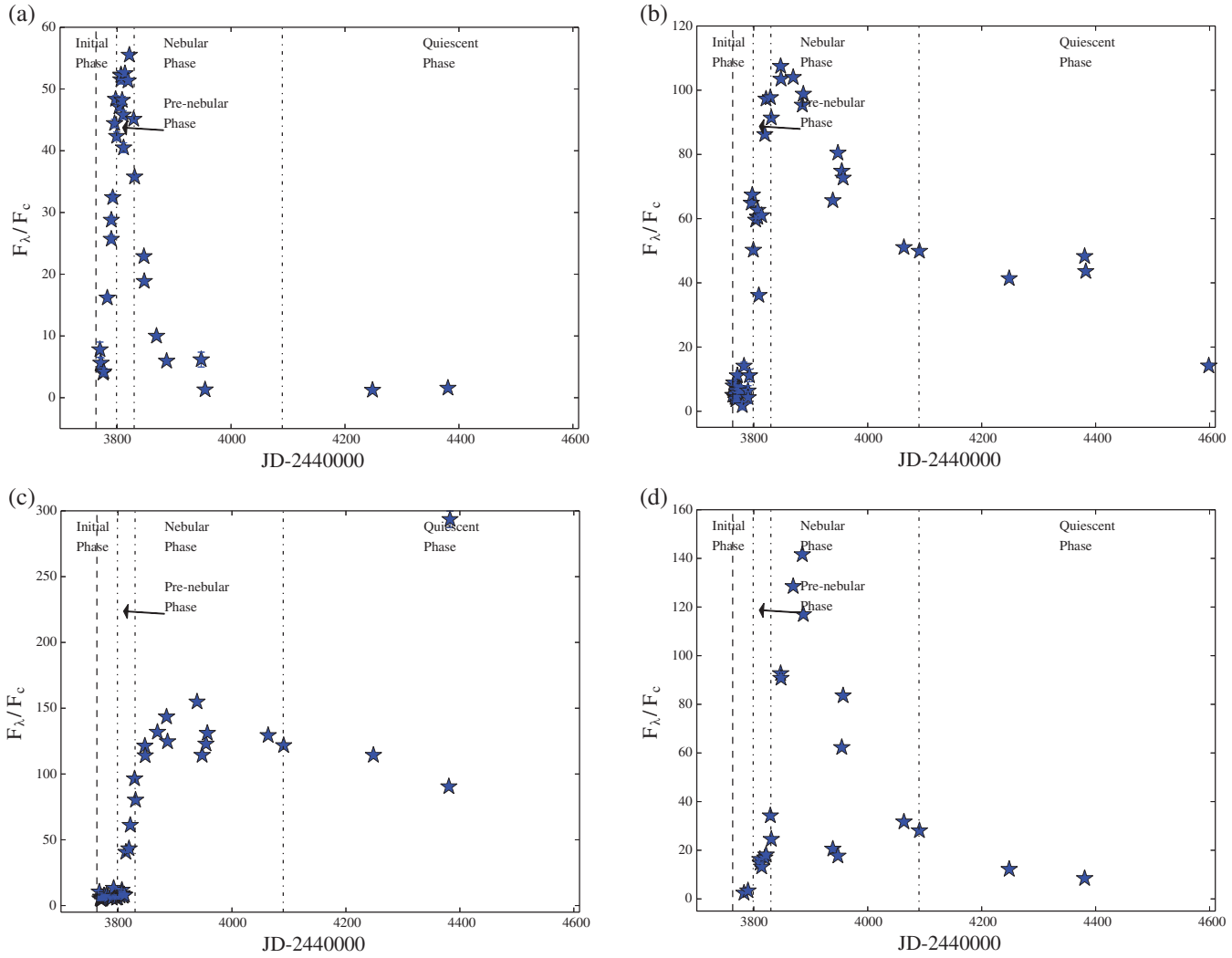

FIGURE 7 V1668 Cyg line spectral evolution. The dashed line represents the time of visual maximum, and the dash–dotted lines represent the end of the different phases of evolution. (a) O I; (b) N III]; (c) C IV; and, (d) N V

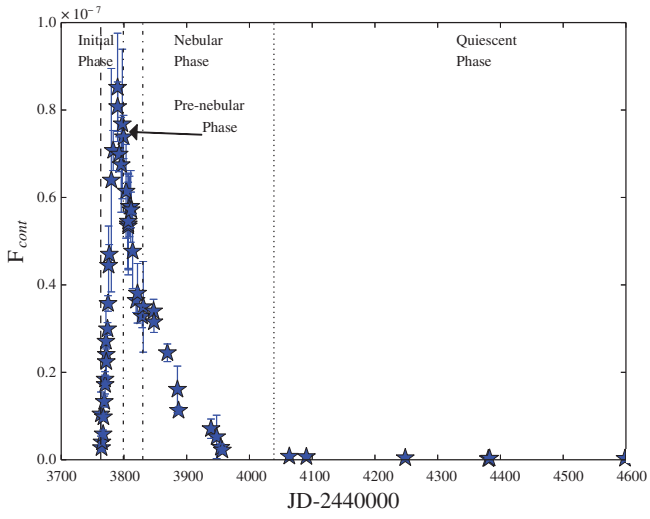

FIGURE 8 V1668 Cyg continuum evolution. See Figure 5a caption

IUE observations, starting on JD 2444248, when the flux of the continuum and emission lines has decreased to 0.5% of the maximum values.

We calculated mass accretion rate for V1668 Cyg in the quiescent phase using Equation 3 and adopting a WD of mass $0.95\,M_\odot$ (Hachisu & Kato 2006) and a radius of $0.0084\,R_\odot$ (determined from Equation 4). The maximum value for the mass accretion rate results $4.8 \pm 0.1 \times 10^{-10}\ M_\odot$ year^{-1}, as determined from the flux of the C IV lines on JD 2444248, about 490 days after the outburst. The average value for the mass accretion rate in the quiescent stage determined from all studied lines in the last four spectra is $1.8 \pm 0.1 \times 10^{-10}\ M_\odot$ year^{-1}. This yields a recurrence time of 2.2×10^5 years, which is consistent with the theoretical accretion time calculated by José & Hernanz (1998) for novae of similar WD mass and expansion speed.

José & Hernanz (1998) identify V1668 Cyg as a CO1 nova based on the agreement between the results of the model and the abundances calculated by Stickland et al. (1981) in the nebular phase or CO4 based on the abundances calculated by Andrea et al. (1994) using observations taken about 338 days after the outburst. These reported abundances are calculated in the nebular phase, while our results are based on averaged dynamical properties through different stages of the outburst.

TABLE 5 PW Vul and V1668 Cyg parameters

Parameter	PW Vul	V1668 Cyg	Reference
M_{WD} ($M_\odot$)	0.83	0.95	(1)
Speed class	Slow	Fast	(2)
L_{max} (erg s^{-1})	$8.1 \pm 0.3 \times 10^{35}$	$2.32 \pm 0.03 \times 10^{36}$	(3)
L_{avg} (erg s^{-1})	$1.0 \pm 0.1 \times 10^{35}$	$4.0 \pm 0.2 \times 10^{35}$	(3)
Average v_{exp} (km s^{-1})	~ 1300	~ 1800	(3)
Average $\dot{M}_{acc}$ ($M_\odot$ year^{-1})	$8.7 \pm 0.4 \times 10^{-10}$	$1.8 \pm 0.1 \times 10^{-10}$	(3)

Notes: M_{WD} is the mass of the white dwarf, L_{max} is the maximum ultraviolet luminosity, L_{avg} is the average ultraviolet luminosity, v_{exp} is the expansion velocity, and $\dot{M}_{acc}$ is the mass accretion rate. References: (1) Hachisu & Kato (2015) for PW Vul and Hachisu & Kato (2006) for V1668 Cyg. (2) Gehrz et al. (1988) for PW Vul and Duerbeck et al. (1980) for V1668 Cyg. (3) This work.

As mentioned in Section 4.1, this difference might be resolved if the model can predict the chemical abundances in the late stages of the outburst.

4.3 | Comparison between the spectral evolution of PW Vul and V1668 Cyg

It can be concluded from the previous results that:

1. V1668 Cyg demonstrated a stronger outburst than PW Vul, with higher L_λ and average expansion speed. This is consistent with the correlation between the speed of the nova and the mass of the WD (Warner 2008). See Table 5 for a comparison between some of the parameters of both novae.
2. The maximum and average values for $\dot{M}_{acc}$ were higher for PW Vul in the quiescent phase; this is because $\dot{M}_{acc}$ is inversely proportional to the mass of the primary (see Equation 3).
3. PW Vul average ejection speed and accretion rate in quiescence puts it close to the CO2 model calculated by José & Hernanz (1998), while the average ejection speed and accretion rate of V1668 Cyg place it closer to the CO3 model. The adopted masses of the primaries of the two systems are consistent with this.

5 | CONCLUSION

In this study, we present the results of two classical novae (PW Vul and V1668 Cyg), and the main conclusions can be summarized as follows:

1. The difference between the WD masses (0.83 $M_\odot$ for PW Vul and 0.95 $M_\odot$ for V1668 Cyg) is the main cause behind the difference in the speed class and the spectral evolution of the two novae.
2. The evolutionary curves of the normalized flux (F_λ/F_c) for most of the lines are similar to the evolutionary curves of the absolute flux (F_λ).
3. The difference in the evolutionary curves of F_λ/F_c between different lines is due to the difference in the ionization states and the variation in the density and opacity of the ejecta in different phases of the outburst.
4. Average expansion speeds, masses, and average mass accretion rates in quiescence suggest that both novae lie between CO2 and CO3 models of José & Hernanz (1998).
5. The evolutionary curve of the short wavelength continuum is similar to the evolutionary curve of the continuum at 1455 Å.
6. There is a difference between the models we identified for both novae, using some of the dynamical properties, and the models identified by José & Hernanz (1998). A possible way to resolve this difference is by modifying the model so that it can calculate the chemical abundances in later days of the outburst when these abundances can be determined from nebular line analysis.

ACKNOWLEDGMENTS

This work is based on INES data from the IUE satellite. We thank Dr. Ibrahim Zead for the very helpful discussions. We also thank the anonymous referee for the very useful comments and suggestions.

REFERENCES

Andrea, J., Drechsel, H., & Starrfield, S. 1994, *A&A*, *291*, 869.

Andreae, J., Drechsel, H., Snijders, M. A. J., & Cassatella, A. 1991, *A&A*, *244*, 111.

Andrews, P. J., Lloyd, C., Clements, E. D., et al. 1978, IAU Circ. 3268.

Bath, G. T. 1978, *MNRAS*, *182*, 35.

Cassatella, A., Altamore, A., & González-Riestra, R. 2002, *A&A*, *384*, 1023.

Cassatella, A., Altamore, A., & González-Riestra, R. 2005, *A&A*, *439*, 205.

Cassatella, A., Benvenuti, P., Clavel, J., et al. 1979, *A&A*, *74*, L18.

Cassatella, A., & Gonzalez Riestra, R. 1988, in: *IAU Colloq. 94: Physics of Formation of FE II Lines Outside LTE*, eds. R. Viotti, A. Vittone, & M. Friedjung, Astrophysics and Space Science Library, Vol. *138*, D. REIDEL PUBLISHING COMPANY (Dordrecht), 115.

Downes, R. A., & Duerbeck, H. W. 2000, *AJ*, *120*, 2007.

Duerbeck, H. W. 2008, in: *Classical Novae*, eds. M. F. Bode & A. Evans, 2nd ed., Vol. *43*, Cambridge University Press (Cambridge), 1.

Duerbeck, H. W., Rindermann, R., & Seitter, W. C. 1980, *A&A*, *81*, 157.

Gehrz, R. D., Hackwell, J. A., Grasdalen, G. I., et al. 1980, *ApJ*, *239*, 570.

Gehrz, R. D., Harrison, T. E., Ney, E. P., et al. 1988, *ApJ*, *329*, 894.

González-Riestra, R., & Krautter, J. 1998, in: *Ultraviolet Astrophysics Beyond the IUE Final Archive*, eds. W. Wamsteker, R. Gonzalez Riestra, & B. Harris, ESA Special Publication, Vol. *413*, ESA Publications Division (Noordwijk), 367.

Hachisu, I., & Kato, M. 2006, *ApJS*, *167*, 59.

Hachisu, I., & Kato, M. 2014, *ApJ*, *785*, 97.

Hachisu, I., & Kato, M. 2015, *ApJ*, *798*, 76.

José, J., & Hernanz, M. 1998, *ApJ*, *494*, 680.

Kato, M., & Hachisu, I. 1994, *ApJ*, *437*, 802.

Kosai, H., Takana, W., Watanabe, T., et al. 1984, IAU Circ. 3963.

Loiseau, N., & Solano, E. 1998, in: *Ultraviolet Astrophysics Beyond the IUE Final Archive*, eds. W. Wamsteker, R. Gonzalez Riestra, & B. Harris, ESA Special Publication, Vol. *413*, ESA Publications Division (Noordwijk), 715.

Mclaughlin, D. B. 1945, *PASP*, *57*, 69.

Morrison, W., Beckman, K., Baroni, S., & Cavagna, N. 1978, IAU Circ. 3264.

Nauenberg, M. 1972, *ApJ*, *175*, 417.

Schwarz, G. J., Shore, S. N., Starrfield, S., et al. 2001, *MNRAS*, *320*, 103.

Seaton, M. J. 1979, *MNRAS*, *187*, 73P.

Shore, S. N. 2008, in: *Classical Novae*, eds. M. F. Bode & A. Evans, 2nd ed., Vol. *43*, Cambridge University Press (Cambridge), 194.

Shore, S. N. 2012, *Bulletin of the Astronomical Society of India*, *40*, 185.
Shore, S. N., Sonneborn, G., Starrfield, S., Gonzalez-Riestra, R., & Polidan, R. S. 1994, *ApJ*, *421*, 344.
Slovak, M. H., & Vogt, S. S. 1979, *Nature*, *277*, 114.
Stickland, D. J., Penn, C. J., Seaton, M. J., Snijders, M. A. J., & Storey, P. J. 1981, *MNRAS*, *197*, 107.
Warner, B. 2003, *Cataclysmic Variable Stars*, Cambridge University Press (Cambridge).
Warner, B. 2008, in: *Classical Novae*, eds. M. F. Bode & A. Evans, 2nd ed., Vol. *43*, Cambridge University Press (Cambridge), 16.

How to cite this article: Hamed GM, Sanad MR, Yousef S, Essam A, El Rafy M. Spectral evolution of the two classical novae PW Vul and V1668 Cyg using International Ultraviolet Explorer low-resolution spectra, *Astron. Nachr./AN*. 2018;339:173–182. https://doi.org/10.1002/asna.201813369.